Title Protective effects of rituximab on puromycin-induced apoptosis, loss of adhesion and cytoskeletal alterations in human podocytes

Stefanie Jeruschke
University Hospital Essen
Dana Künzl
University Hospital Essen
Peter Friedrich Hoyer
University Hospital Essen
Stefanie Weber (stefanie.weber@med.uni-marburg.de)
University Hospital Essen

Research Article

Keywords: podocytes, kidney fuction, cytoskeletal alterations, rituximab

Posted Date: May 19th, 2021

DOI: https://doi.org/10.21203/rs.3.rs-534045/v1

Abstract

Background Podocytes are highly specialized cells playing a key role in the filtration function of the kidney. A damaged podocyte ultrastructure is associated with a reorganization of the actin cytoskeleton and accompanied with a loss of adhesion to the glomerular basement membrane leading to proteinuria in many forms of glomerular diseases, e.g. nephrotic syndrome. If the first-line therapy with glucocorticoids fails, alternative immunosuppressive agents are used, which are known to have the potential to stabilize the actin cytoskeleton. A new option for preventing relapses in steroid dependent nephrotic syndrome is the monoclonal antibody rituximab, which, in addition to its B-cell depleting effect, is assumed to have direct effects on podocytes.

Objectives We here provide data on the non-immunological *off-target* effects of the immunosuppressant rituximab on podocyte structure and dynamics in an *in vitro* puromycin aminonucleoside model of podocyte injury.

Methods A conditionally immortalized human podocyte cell line was used. Differentiated podocytes were treated with puromycin aminonucleoside and rituximab. Our studies focussed on analyzing the structure of the actin cytoskeleton, cellular adhesion and apoptosis using immunofluorescence staining and protein biochemistry methods.

Results Treatment with rituximab resulted in a stabilization of podocyte actin stress fibers in the puromycin aminonucleoside model, leading to an improvement in cell adhesion. A lower apoptosis rate was observed after parallel treatment with puromycin aminonucleoside and rituximab visualized by reduced nuclear fragmentation. Consistent with this data Western-blot analyses demonstrated that rituximab directly affects the caspase pathways by inhibiting the activation of Caspases-8 and − 3, suggesting that rituximab may inhibit apoptosis.

Conclusions In conclusion, our results indicate an important role of the immunosuppressant rituximab in terms of stability and morphogenesis of podocytes, involving apoptosis pathways. This could help to improve therapeutical concepts for patients with proteinuria mediated by diseased podocytes.

Key Points

Puromycin aminonucleoside induced injury of human podocytes *in vitro* was partially prevented with rituximab, leading to a stabilization of podocyte actin stress fibers, an improvement in cell adhesion and a reduced apoptosis rate.

1. Introduction

The renal filtration barrier consists of fenestrated endothelial cells, the glomerular basement membrane (GBM) and podocytes [1-2]. This complex structure ensures the selective ultrafiltration of plasma. Podocytes are terminally differentiated visceral glomerular epithelial cells forming the final barrier to

urinary protein loss by means of foot processes and interposed slit diaphragms [3]. To maintain an intact glomerular filter the foot processes are linked to the GBM via a3/b1 integrins and dystroglycans and contain an actin-based cytoskeleton together with actin-associated proteins such as synaptopodin [4]. All these components are essential to prevent the development of proteinuria, defined as the leckage of protein from the blood to the urinary compartment, which occurs in many forms of glomerular diseases. Injury of podocytes leads to fusion of filtration slits, apical displacement or disruption of the slit diaphragm and foot process effacement which is based on rearrangements of the actin cytoskeleton of the involved foot processes [5]. If these structural changes in podocyte morphology occur early, they are fully reversible and the foot processes reorganize within minutes due to their high dynamics. In contrast, persistence of podocyte injury as e.g. found in steroid resistent nephrotic syndrome (NS) can cause podocyte detachment from the GBM and cell death associated with development of proteinuria and with permanent deterioration of the glomerular filter [6].

The incidence of idiopathic NS in children is 2-7 / 100.000 children. Patients present with sudden onset of proteinuria, hypoalbuminaemia, edema and progression to end-stage renal diesease. However the exact pathogenesis of NS is unknown. Most children with idiopathic NS respond to the initial therapy with corticosteroids, but more complicated forms, such as frequently relapsing NS and steroid dependent or steroid resistant NS, need corticosteroid sparing, second line drugs, e.g. immunosuppressive agents such as cyclosporine A or cyclophosphamide [7-8]. Most affected children are helped by these drugs, but 10-20% of these cases do not completely respond to immunosuppressant treatment [9-10]. Experimental findings show that immunosuppressants may have direct effects on podocytes that are independent of their immunomodulatory effects [11-14]. However, the exact non-immunological mechanisms are yet not clear.

A new treatment option for NS is rituximab (RTX). It has been shown to be effective in the therapy of patients with complicated NS [15-18]. CD20, normally expressed on B-lymphocytes, is the known binding partner of RTX, a chimeric monoclonal antibody, inhibiting CD20-mediated B-cell proliferation [19]. It was developed for the treatment of B-cell non-Hodgkin's lymphoma and antibody-mediated autoimmune diseases [20-21]. Previous data have shown that RTX is also able to affect / stabilize the kidney filtration barrier in a B-cell independent manner as a direct modulator of podocyte function. Fornoni reported a direct binding of RTX to sphingomyelin phosphodiesterase acid like 3b (SMPDL3B), thereby directly acting on podocyte function [12].

In the present study we analysed these *off-target* effects of the immunosuppressant RTX in a B-lymphocyte independent *in vitro* cell-culture model of human podocytes. Treatment with RTX was performed in a puromycin aminonucleoside (PAN) experimental model of podocyte injury to analyse actin structure, cellular adhesion and mechanisms of apoptosis by means of cell imaging and protein biochemistry studies. We provide direct evidence that PAN induced disruption of the actin cytoskeleton was prevented by RTX. This was associated with an improvement in cell adhesion. Furthermore PAN-induced apoptosis, visualized by cell nucleus fragmentation, was prevented with RTX. Western-blot

analyses confirmed, that RTX reduced apoptosis by affecting the caspase pathway via inhibiting the activation of caspases-8 and -3.

We present data demonstrating *off-targets* effects of RTX proposing that mechanisms of anoikis (apoptosis by lack of cell-matrix attachment) and cytoskeleton reorganization are modulated by RTX.

2. Materials And Methods

Cell Culture

Conditionally immortalized human podocytes were generated by Prof. Dr. Moin A. Saleem (University of Bristol, South Mead Hospital, Bristol, UK) [22]. Culture conditions were described previously [22].

Experimental Design and Drug Treatment

In order to examine the non-immunological effects of RTX on PAN induced cytoskeletal defects, podocytes were grown under growth restrictive conditions for 12 days and subsequently incubated with media containing 10 % FBS in the presence of 30 µg / ml PAN (Sigma, Munich, Germany), 100 µg / ml MabThera® (Roche, Basel, Switzerland) or the combination of both for 48 hours. All experiments were performed at least three times starting on growth-restricted days 12–14 (methodology previously described in [13]).

RNA isolation from cells

Total RNA was isolated using the RNeasy Mini Kit (Qiagen, Hilden, Germany) according to the manufacturer's instructions including DNase digestion.

RT-PCR analysis

1–2 µg of total RNA was reverse transcribed with random hexamers and the SuperScript III First-Strand Synthesis System for RT-PCR (Invitrogen, Karlsruhe, Germany) according to the manufacturer's instructions.

RT-PCR for *MS4A1* was performed according to the manufacturer's instructions using the TaqMan Gene Expression Assay HS00544819_m1 (Applied Biosystems, Darmstadt, Germany) in combination with the TaqMan Fast Universal PCR Master Mix (Applied Biosystems, Darmstadt, Germany). RT-PCR was performed with a StepOnePlus engine (Applied Biosystems, Darmstadt, Germany) (methodology previously described in [23]).

Apoptosis Detection

Hoechst 33342-staining of podocytes was performed as previously described [24]. Images were obtained by a Zeiss Axio Imager A1 fluorescence microscope and Axio Vision SE64 Rel. 4.9.1 software (Zeiss,

Jena, Germany). Apoptosis was defined as percentage of cells with nuclear fragmentation. For each sample in a given experiment, at least 200 randomly chosen cells were analyzed.

Immunofluorescence and cell imaging

For immunofluorescence, podocytes were plated on glass coverslips. After treatment, cells were fixed with 4 % formaldehyde (Fischar, Saarbrücken, Germany) for 15 min at 37°C, washed with PBS and permeabilized with PBS / 0.5 % Triton X-100 / 3 % BSA for 45 min at room temperature. After washing with blocking buffer (PBS / 0.5 % BSA), cells were incubated with Alexa Fluor™ 488 phalloidin (1:1000, Thermo Fisher Scientific, Waltham, USA) for actin staining in blocking buffer for 1 hour at room temperature (methodology previously described in [13]). In parallel, nuclei were stained with 4.6-diamidino-2-phenylindole dihydrochloride (DAPI, Sigma, Munich, Germany).

Fluorescence imaging was performed on a Zeiss Axio Imager A1 Fluorescence microscope with Axio Vision SE64 Rel. 4.9.1 software (Zeiss, Jena, Germany). Images were acquired using 10× and 20× phase contrast objectives with appropriate filter sets. Image processing and analysis was performed with ImageJ (https://imagej.nih.gov/ij/) software. All images were acquired at random positions.

Cell Adhesion Assay

After 48 hours of pharmacological treatment human podocytes were detached using Trypsin-EDTA (Biochrom, Berlin, Germany) and seeded on glass-coverslips in a 24-well plate for adhesion tests. After 1 and 6 hours, cells were fixed with 4 % formaldehyde (Fischar, Saarbrücken, Germany) and staining of the actin cytoskeleton was carried out as described above. For each condition the degree of spreading of 300 randomly chosen cells was measured using region measurement tools in ImageJ software (https://imagej.nih.gov/ij/).

Western Blot Analysis

Cells were harvested using CelLytic MT-buffer (Sigma-Aldrich, Hamburg, Germany) according to manufacturer's instructions. Lysis-buffer was supplemented with Protease Inhibitor Cocktail (Sigma-Aldrich, Hamburg, Germany), 10 µg / ml aprotinin (Roche, Mannheim, Germany), 10 µg / ml leupeptin (Roche, Mannheim, Germany) and 2 mM phenylmethanesulfonylfluoride (PMSF, Sigma, Munich, Germany). Isolation was performed at 4°C. Total protein content was measured by Bio-Rad protein assay (Bio.Rad, Munich, Germany). Samples (each 15 µg protein) were supplemented with Laemmli sample buffer (Bio-Rad, Munich, Germany) and boiled for 10 min at 95°C (methodology previously described in [23]).

Proteins were separated using 12 % Mini-PROTEAN TGX Precast Gels (Bio-Rad, Munich, Germany) and transferred on 0.45 µm PVDF Transfer Membranes (Thermo Scientific, Schwerte, Germany) with a MiniProtean Tetra Cell electrophoresis system (Bio-Rad, Munich, Germany) and a Biometra fastblot B34 blotting device (Biometra, Göttingen, Germany). 15 µl Precision Plus Protein All Blue Standard (Bio-Rad,

Munich, Germany) was used as marker. Membranes were incubated with primary antibodies against CD20 (MabThera®: 1:100; Roche, Basel, Switzerland), Caspase-3 (1:5000; Cell Signaling, Danvers, USA), cleaved Caspase-3 (1:5000; Cell Signaling, Danvers, USA), Caspase 8 (1:5000; Cell Signaling, Danvers, USA) or cleaved Caspase-8 (1:1000; Cell Signaling, Danvers, USA). Secondary antibodies used were horseradish peroxidase-conjugated goat anti-human IgG (Santa Cruz, Heidelberg, Germany: 1:10000 against MabThera®), goat anti-rabbit IgG (Santa Cruz, Heidelberg, Germany; 1:10000 against Caspase-3 / cleaved Caspase-3 and cleaved Caspase-8) and goat anti-mouse IgG (Santa Cruz, Heidelberg, Germany; 1:10000 against Caspase-8). Signal detection was performed with SuperSignal West Femto Chemiluminescent Substrate (Thermo Scientific, Schwerte, Germany) and visualized by the FUSION FX7 chemiluminescence-system (PEQLAB, Erlangen, Germany) und Fusion-software (PEQLAB, Erlangen, Germany). Intensity of signals was determined using ImageJ software (https://imagej.nih.gov/ij/). Densitometric data of the cleaved Caspase antibodies were normalized to full-length Caspase proteins (methodology previously described in [23]).

Statistical analysis

Values from multiple experiments were expressed as means ± SD. Statistical analysis was performed with GraphPad Prism 6.0 using Kruskal-Wallis test (non-parametric one-way ANOVA) with Dunn's multiple comparisons test or an ordinary one-way ANOVA with Tukey's multiple comparisons test. Statistical significance was defined as $p < 0.05$.

3. Results

Human podocytes do not express CD20

To study possible *off-target* effects of RTX, we first excluded the expression of CD20 on human podocytes. CD20 is the known binding partner of RTX and a surface antigen from the MS4A family, encoded by the gene *MS4A1* [25]. Peripheral blood mononuclear cells were used as a positive control for the analysis of *MS4A1* / CD20 expression on podocytes. These are composed of monocytes, natural killer cells and lymphocytes and express CD20 antigen [26]. RT-PCR- and Western-blot analysis confirmed, that podocytes do not express *MS4A1* on the RNA level as well as CD20 on the protein level (Fig1), so that a different, unknown pathway (*off-target* effect) of RTX on podocytes has to be assumed.

RTX prevents disruption of the actin cytoskeleton

Different studies of human podocytes indicated direct effects of immunosuppressive agents on the podocyte cytoskeleton besides their previously suggested immunosuppressive actions [11-14].

To study possible effects on podocyte morphology, we applied puromycin aminonucleoside (PAN) as a well-recognized *in vitro* model of podocyte injury. Podocyte actin stress fibers, playing an important role in the proper function of the filtration barrier [27], were analyzed in a semi-quantitative manner with respect to a possible rescue effect of RTX.

For this, cells were divided semi-quantitatively into the categories "healthy actin stress fiber appearance", "reduced number of actin stress fibers" and "no actin stress fibers". Untreated control cells exhibited a healthy actin cytoskeleton in 89.6 % of the podocytes, 7.6 % contained a reduced number of actin stress fibers and in 2.8 % no actin stress fibers were visible (Fig2, Table 1). As expected, treatment with PAN (30 µg / ml for 48 hours) caused strong morphological and cytoskeletal defects. PAN led to less and smaller cells (data not shown, see [13]), to a significant increase in cells without actin stress fibers (PAN: 87.7 % vs. Controls: 2.8 %; $p < 0.0001$) and to a decrease in cells with healthy actin stress fibers (PAN: 2.0 % vs. Controls: 89.6 %; $p < 0.0001$). When exposed to RTX (100 µg / ml) in combination with PAN number of podocytes with healthy actin stress fibers significantly increased (PAN + RTX: 10.0 % vs. PAN: 2.0 %; $p < 0.05$), while cells without actin stress fibers decreased (PAN + RTX: 75.9 % vs. PAN: 87.7 %; $p < 0.01$). Interestingly, RTX alone did not affect podocyte morphology or the actin cytoskeleton, showing almost similar results to non-exposed control cells. This suggests that RTX might specifically act on signaling pathways altered in podocyte damage.

RTX prevents podocyte apoptosis

An increasing number of reports confirmed that PAN induces apoptosis in podocytes and that coincubation with different immunosuppressants protects podocytes from undergoing apoptosis [13, 28-29]. As we recently observed podocyte loss following PAN treatment [13], we tested whether this massive decrease in cell number was due to apoptosis and if RTX has a protective effect on apoptosis induction.

The process of apoptosis results in nuclear fragmentation, reduction in cell volume and a change in cell shape with vesicle formation [30]. In order to determine the effect of RTX on PAN-induced apoptosis, DNA fragmentation was quantified by staining cell nuclei with Hoechst 33342 and analyzing their shape. Cells with fragmented nuclei were defined as apoptotic cells. In control cells, 99.4 % of nuclei appeared normal (Fig3, Table 2). Treatment with RTX for 48 hours showed neither a positive nor a negative effect on apoptosis and resulted in cells with less than 1 % fragmented nuclei. In agreement with recent data [13, 24] PAN treatment led to a significant induction of apoptosis as the number of cells with fragmented DNA increased to 22.6 % ($p < 0.0001$; PAN vs. Controls). Combining PAN treatment with RTX led to a significant reduction of apoptosis (11.9 % apoptotic cells as compared to PAN treatment alone ($p < 0.0001$; PAN + RTX vs. PAN)).

The caspase cascade is critical in mediating apoptosis: The initiator Caspase-8 is part of the extrinsic apoptosis pathway and activates directly Caspase-3, the final downstream protein required for apoptosis. To determine whether caspases underlie PAN-induced apoptosis of podocytes and whether the antiapoptotic effect of RTX involves suppression of caspase activation, we performed Caspase-8 and -3 Western-blots. The initiator Caspase-8 is part of the extrinsic pathway of apoptosis activation. It is able to activate apoptosis directly via Caspase-3, one of the final downstream proteins required for apoptosis.

Our results demonstrated that PAN damage significantly increased the activity of Caspase-8 ($p < 0.01$; PAN vs. Controls) and Caspase-3 ($p < 0.05$; PAN vs. Controls) (Table 3, Fig4). In contrast, co-treatment of PAN with RTX was able to reduce the activation levels of both caspases (cleaved Caspase-8: $p < 0.01$;

PAN + RTX vs. PAN / cleaved Caspase-3: $p < 0.05$; PAN + RTX vs. PAN), showing apoptosis levels corresponding to healthy controls and RTX-treated cells.

These results clearly demonstrated that podocyte apoptosis induced by PAN is caspase-dependent and is mediated by the extrinsic pathway through Caspase-8 and -3 activation. The combination of PAN with RTX caused activity levels of the cleaved caspases similar to that of control podocytes, concluding that RTX acts as an anti-apoptotic factor for this cell population.

RTX enhances podocyte adhesion

As a result of NS, podocytes detach from the GBM [6] by losing their cell adherence. The reduction in cell body size following PAN treatment (see [13]) suggested defects in cellular adhesion. Therefore the question arose whether RTX has a protective or regenerative effect on cell adhesion. Thus, cells were detached 48 hours after treatment with RTX, PAN or PAN + RTX and we quantified adhesion efficiency by measuring their size at 1 and 6 hours post-plating on glass coverslips.

Fig5a shows representative podocytes stained with DAPI and phalloidin, 1 and 6 hours after post-plating: Cell size differed depending on treatment and time points (Fig5b; Table 4). 1 hour after post-plating the average cell size of a control podocyte was 6860 μm^2. Cells treated exclusively with RTX showed a similar mean cell size of 6580 μm^2. Treatment with PAN resulted in a significant decrease in cell size to 4285 μm^2 ($p < 0.0001$; PAN vs. Controls). In contrast, the simultaneous treatment with PAN and RTX resulted in an almost complete rescue of cell size ($p < 0.0001$; PAN + RTX: 6343 μm^2 vs. PAN: 4285 μm^2). As expected, cells were larger after 6 hours post-plating (Controls: 12562 μm^2) than after 1 hour (Controls: 6860 μm^2). PAN treatment resulted in a 57.4 % reduction in cell size ($p < 0.0001$; PAN: 5350 μm^2 vs. Controls: 12562 μm^2). In contrast the combined treatment PAN + RTX led to a significant rescue in cell size even after 6 hours ($p < 0.0001$; PAN + RTX: 10173 μm^2 vs. PAN: 5350 μm^2).

In summery we were able to confirm that PAN treated podocytes adhered and spread less efficiently as compared to control cells. However, when cells were treated with PAN and RTX, the lack of adhesion efficiency was recovered substantially.

4. Discussion

Historically, the cause of NS associated with proteinuria has been discussed to reside in defective T-cell function [31]. Today there is much evidence that the disease is of heterogeneous origin and that podocytes are directly involved in the pathogenesis. Podocyte damage causes a reorganization of the complex actin cytoskeleton, leading to an effacement and detachment of foot processes from the GBM (loss of adhesion) and, in the case of chronic damage, to apoptosis [6]. Patients who do not respond to steroids or show severe side effects when exposed to excessive glucocorticoid therapy may be treated with steroid sparing, immunosuppressive substances such as cyclosporin A or cyclophosphamide [7-8, 10, 32]. However, these drugs do not always prevent relapses or show unacceptable side effects. For this

reason, alternative, more effective concepts to reduce glucocorticoid toxicity have been developed. A nowadays frequently used candidate is the monoclonal antibody rituximab (RTX) [33]. RTX binds to CD20 on human B-lymphocytes and leads to B-cell depletion via complement-mediated, antibody-dependent and antiproliferative effects [20]. Regarding NS, Ravani et al. carried out a multicentre open-label randomized controlled trial in children with steroid dependent NS who were either treated with prednisone alone or in combination with RTX. They were able to show that RTX-treated children had a 42 % reduction in proteinuria after three months of treatment and overcome a longer period without relapses [34]. Numerous other clinical studies provided similar findings [9, 35-38]. These results suggested that RTX could be an effective steroid saving therapy for children with NS.

The potential beneficial effect of RTX in the treatment of proteinuria, as well as no exclusive evidence of B-lymphocyte involvement in Ravani's study, in which children remained in remission despite B-cell recurrence [34], led to the hypothesis that RTX may have a direct protective effect on podocyte function. This prompted us to investigate possible effects of RTX on podocytes in an *in vitro* experimental model of podocyte injury.

We were able to show that RTX reduces podocyte damage in an experimental model of NS independent of its immunosuppressive effects. RTX protects podocytes from apoptosis, stabilizes actin stress fibers and leads to improved adhesion properties.

The damage model we selected was puromycin aminonucleoside (PAN), a toxic molecule used experimentally in animals to induce proteinuria [39-40]. It changes the podocyte actin cytoskeleton, accompanied by an effacement of their foot processes, and thus represents a common model for glomerular diseases under experimental conditions [41]. The use of PAN on isolated podocytes induces alterations that are supposed to mimic NS, independent of immune cells. Therefore it is a suitable model for studying the effects of RTX independently of B-cell modulation. Together with the observation that the strong podocyte damage caused by PAN can also be reduced by a wide variety of pharmacological substances [13, 42-43] we chose this model for studying the decisive effects of the immunosuppressant RTX on cytoskeletal alterations, cell adherence and apoptosis.

Here we show that PAN induced morphological and cytoskeletal alterations with an almost complete loss of the actin stress fibers. A related mechanism *in vivo* is the detachment of podocytes from the GBM, which in addition to the actin cytoskeleton ensures stable anchoring of the podocytes. The importance of cell adhesion can be seen in diseases with a defect in adhesion receptors, linking the podocytes to the GBM. For example, patients homozygous for mutations in the *integrin α3* gene, *ITGA3*, have disrupted basement membrane structures and compromised barrier functions and develop congenital nephrotic syndrome [44]. In a PAN-induced model of NS, rats show urinary podocytes, due to podocyte detachment. This effect was also confirmed in human studies involving proteinuric patients [45-46]. Therefore, loss of adhesion was considered as an important feature for PAN-induced injury in our study. PAN treatment resulted in a significant reduction in podocyte cell size after post-plating, which was used as a parameter of cell adhesion. Goto et al. assumed that PAN treatment in rats effects the actin binding protein alpha-

actinin, interacting with the adhesion complexes of the GBM [47]. Here, the loss of podocyte adhesion was directly related to massive cytoskeletal alterations. Different studies have additionally implicated increased apoptosis of podocytes in patients with glomerular diseases [48-50]. Based on these findings, we analyzed the number of fragmented cell nuclei in human podocytes as a measure of apoptosis. Similar to previous studies on human podocytes [13, 46], we demonstrated that PAN leads to apoptosis. In addition, the increased number of fragmented cell nuclei correlated with an activation of the extrinsic caspase cascade (increased cleaved Caspase-8 and -3 expression).

Finally, we were able to show that the addition of rituximab is protective against these numerous described effects of PAN on human podocytes.

Fornoni et al. demonstrated an effect of RTX on podocytes via binding to SMPDL3B, independent of the CD20 epitope on B-lymphocytes. The administration of RTX is associated with a reduced incidence of recurrent NS and accompanied with an upregulation of SMPDL3B, normally expressed significantly less in these patients [12]. This has also been confirmed *in vivo* [51].

In addition to stabilizing the actin cytoskeleton, RTX has a positive effect on cell adhesion in our study. Parallel treatment of podocytes with PAN and RTX is associated with an almost complete rescue of cell size, demonstrating an improvement in cell adhesion. This hypothesis is supported by the study of Cittera et al. demonstrating the induction of cell aggregates in a B-lymphoma cell line by RTX [52]. Because RTX stabilizes the actin cytoskeleton and improves cell adhesion, the question arises whether the cytoskeletal alterations are related to cell adhesion: The detachment of podocytes from the GBM *in vivo* takes place in different stages. First, podocytes lose their foot process connections to the GBM, while foot processes of neighboring podocytes are still connected. However, if one podocyte is damaged, other podocytes also initiate structural and functional changes. The most important alteration is the effacement of the foot processes [53]. This effacement is probably due to podocytic stress and precedes cell detachment from the GBM. Transmission electron micrographs taken during the detachment process showed podocytes with flattened foot processes [54]. Nevertheless, it remains unclear which events lead to alterations in the actin cytoskeleton and to podocyte detachment and whether these occur simultaneously.

In literature the effects of RTX on apoptosis are discussed controversially, depending on the cell lines used. While some authors attribute a pro-apoptotic effect of RTX in B-lymphoma cell lines [55-56], others were not able to detect apoptosis induced by RTX [52, 57]. Interestingly, RTX did not lead to caspase activation in these models [55, 57]. In our study RTX alone showed no pro-apoptotic effects on podocytes, whereas the addition of RTX to PAN-treated cells was associated with a significant reduction in apoptosis. This was accompanied with a reduced activation of the caspase cascade (decreased cleaved Caspase-8 and -3 expression). In line with our data, a study on radiation-induced nephropathy reports attenuated caspase-3 activation when podocytes were pretreated with RTX prior to radiation [58].

The fact that RTX has a protective effect on cell adhesion as well as on apoptosis suggests a special apoptosis mechanism based on the loss of adhesion, named anoikis [59]. Caspase-8 is, despite its well-known role as apoptosis initiator, part of signaling cascades responsible for cell adhesion [60-61]. Since

we were able to show a connection between RTX and the caspase cascade, it would be conceivable that RTX reduces apoptosis and improves adhesion through a reduced activation of Caspase-8. The extent to which cell adhesion loss and apoptosis influence each other in RTX treatment has to be examined in further studies.

In summary, we were able to show that RTX treatment of PAN-treated podocytes in cell culture significantly reduce podocyte damage and lead to reduced apoptosis, increased cell adhesion and a stabilization of the actin cytoskeleton. We suggest that these effects play a potential role in the treatment of NS, independent of B-cell function.

Declarations

Funding: SJ received funding from the CV Wissenschaftsförderung Essen und DK from ELAN (Essener Ausbildungsprogramm "Labor und Wissenschaft" für den aerztlichen Nachwuchs).

Conflicts of interest/Competing interests: All authors declare that they have no conflict of interest.

Ethics approval: Not applicable.

Consent to participate: Not applicable.

Consent for publication: Not applicable.

Availability of data and material: Under request.

Code availability: Not applicable.

Author contributions: Stefanie Jeruschke and Stefanie Weber contributed to the study conception and design. Material preparation, data collection and analysis were performed by Dana Künzl and Stefanie Jeruschke. The first draft of the manuscript was written by Stefanie Jeruschke and all authors commented on previous versions of the manuscript. All authors read and approved the final manuscript.

Acknowledgments

The authors thank Ralf Herrmann for his help in conducting the statistical analysis.

References

1. Brenner BM, Hostetter TH, Humes HD. Molecular basis of proteinuria of glomerular origin. N Engl J Med. 1978; 298(15):826-33.
2. Rennke HG, Venkatachalam MA.Glomerular permeability of macromolecules. Effect of molecular configuration on the fractional clearance of uncharged dextran and neutral horseradish peroxidase in the rat. J Clin Invest. 1979; 63(4):713-7.

3. Asanuma K, Yanagida-Asanuma E, Takagi M, Kodama F, Tomino Y. The role of podocytes in proteinuria. Nephrology (Carlton). 2007; Suppl 3:S15-S20.
4. Barisoni L, Mundel P. Podocyte biology and the emerging understanding of podocyte diseases. Am J Nephrol. 2003; 23(5):353-60.
5. Shankland SJ. The podocyte's response to injury: role in proteinuria and glomerulosclerosis. Kidney Int. 2006; 69(12):2131-47.
6. Mundel P, Reiser J. Proteinuria: an enzymatic disease of the podocyte? Kidney Int. 2010; 77:571-80.
7. Büscher AK, Kranz B, Büscher R, Hildebrandt F, Dworniczak B, Pennekamp P, Kuwertz-Bröking E, Wingen AM, John U, Kemper M, Monnens L, Hoyer PF, Weber S, Konrad M. Immunosuppression and renal outcome in congenital and pediatric steroid-resistant nephrotic syndrome. Clin J Am Soc Nephrol. 2010; 5(11):2075-84.
8. Büscher AK, Beck BB, Melk A, Hoefele J, Kranz B, Bamborschke D, Baig S, Lange-Sperandio B, Jungraithmayr T, Weber LT, Kemper MJ, Tönshoff B, Hoyer PF, Konrad M, Weber S; German Pediatric Nephrology Association (GPN). Rapid Response to Cyclosporin A and Favorable Renal Outcome in Nongenetic Versus Genetic Steroid-Resistant Nephrotic Syndrome. Clin J Am Soc Nephrol. 2016; 11(2):245-53.
9. Iijima K, Sako M, Nozu K. Rituximab Treatment for Nephrotic Syndrome in Children. Curr Pediatr Rep. 2015; 3(1):71-7.
10. Wang X, Xu H. New insights into treatment of nephrotic syndrome in children. Contrib Nephrol. 2013; 181:119-30.
11. Faul C, Donnelly M, Merscher-Gomez S, Chang YH, Franz S, Delfgaauw J, Chang JM, Choi HY, Campbell KN, Kim K, Reiser J, Mundel P. The actin cytoskeleton of kidney podocytes is a direct target of the antiproteinuric effect of cyclosporine A. Nat Med. 2008; 14(9):931-8.
12. Fornoni A, Sageshima J, Wei C, Merscher-Gomez S, Aguillon-Prada R, Jauregui AN, Li J, Mattiazzi A, Ciancio G, Chen L, Zilleruelo G, Abitbol C, Chandar J, Seeherunvong W, Ricordi C, Ikehata M, Rastaldi MP, Reiser J, Burke GW 3rd. Rituximab targets podocytes in recurrent focal segmental glomerulosclerosis. Sci Transl Med. 2011; 3(85):85ra46.
13. Jeruschke S, Buescher AK, Oh J, Saleem MA, Hoyer PF, Weber S, Nalbant P. Protective effects of the mTOR inhibitor everolimus on cytoskeletal injury in human podocytes are mediated by RhoA signaling. PLoS One. 2013; 8:e55980.
14. Yoo TH, Fornoni A. Nonimmunologic targets of immunosuppressive agents in podocytes. Kidney Res Clin Pract. 2015; 34(2):69-75.
15. Benz K, Dotsch J, Rascher W, Stachel D. Change of the course of steroid-dependent nephrotic syndrome after rituximab therapy. Pediatr Nephrol. 2004; 19(7):794-7.
16. Gulati A, Sinha A, Jordan SC, Hari P, Dinda AK, Sharma S, Srivastava RN, Moudgil A, Bagga A. Efficacy and safety of treatment with rituximab for difficult steroid-resistant and -dependent nephrotic syndrome: multicentric report. Clin J Am Soc Nephrol. 2010; 5(12):2207-12.

17. Otukesh H, Hoseini R, Rahimzadeh N, Fazel M. Rituximab in the treatment of nephrotic syndrome: a systematic review. Iran J Kidney Dis. 2013; 7(4):249-56.
18. Popko K, Górska E, Kuźma-Mroczkowska E. Effectiveness of rituximab in nephrotic syndrome treatment. Cent Eur J Immunol. 2017; 42(3):313-17.
19. Smith MR. Rituximab (monoclonal anti-CD20 antibody): mechanisms of action and resistance. Oncogene. 2013; 22(47):7359-68.
20. Selewski DT, Shah GV, Mody RJ, Rajdev PA, Mukherji SK. Rituximab (Rituxan). AJNR Am J Neuroradiol. 2010; 31(7):1178-80.
21. Edwards JC, Cambridge G. B-cell targeting in rheumatoid arthritis and other autoimmune diseases. Nat Rev Immunol. 2006; 6(5):394-403.
22. Saleem MA, O'Hare MJ, Reiser J, Coward RJ, Inward CD, Farren T, Xing CY, Ni L, Mathieson PW, Mundel P. A conditionally immortalized human podocyte cell line demonstrating nephrin and podocin expression. J Am Soc Nephrol. 2002; 13(3):630-8.
23. Jeruschke S, Jeruschke K, DiStasio A, Karaterzi S, Büscher AK, Nalbant P, Klein-Hitpass L, Hoyer PF, Weiss J, Stottmann RW, Weber S. Everolimus Stabilizes Podocyte Microtubules via Enhancing TUBB2B and DCDC2 Expression. PLoS One. 2015; 10(9):e0137043.
24. Kummer S, Jeruschke S, Wegerich LV, Peters A, Lehmann P, Seibt A, Mueller F, Koleganova N, Halbenz E, Schmitt CP, Bettendorf M, Mayatepek E, Gross-Weissmann ML, Oh J. Estrogen receptor alpha expression in podocytes mediates protection against apoptosis in-vitro and in-vivo. PLoS One. 2011; 6(11):e27457.
25. Cragg MS, Walshe CA, Ivanov AO, Glennie MJ. The biology of CD20 and its potential as a target for mAb therapy. Curr Dir Autoimmun. 2005; 8:140-174.
26. Corkum CP, Ings DP, Burgess C, Karwowska S, Kroll W, Michalak TI. Immune cell subsets and their gene expression profiles from human PBMC isolated by Vacutainer Cell Preparation Tube (CPT) and standard density gradient. BMC Immunol. 2015; 16:48.
27. Greka A, Mundel P. Cell biology and pathology of podocytes. Annu Rev Physiol. 2012; 74:299-323.
28. Takeuchi S, Hiromura K, Tomioka M, Takahashi S, Sakairi T, Maeshima A, Kaneko Y, Kuroiwa T, Nojima Y. The immunosuppressive drug mizoribine directly prevents podocyte injury in puromycin aminonucleoside nephrosis. Nephron Exp Nephrol. 2010; 116(1):e3-10.
29. Shen X, Jiang H, Ying M, Xie Z, Li X, Wang H, Zhao J, Lin C, Wang Y, Feng S, Shen J, Weng C, Lin W, Wang H, Zhou Q, Bi Y, Li M, Wang L, Zhu T, Huang X, Lan HY, Zhou J, Chen J. Calcineurin inhibitors cyclosporin A and tacrolimus protect against podocyte injury induced by puromycin aminonucleoside in rodent models. Sci Rep. 2016; 6:32087.
30. Atale N, Gupta S, Yadav UC, Rani V. Cell-death assessment by fluorescent and nonfluorescent cytosolic and nuclear staining techniques. J Microsc. 2014; 255(1):7-19.
31. Koyama A, Fujisaki M, Kobayashi M, Igarashi M, Narita M. A glomerular permeability factor produced by human T cell hybridomas. Kidney Int. 1991; 40(3):453-60.

32. Liu Y, Yang R, Yang C, Dong S, Zhu Y, Zhao M, Yuan F, Gui K. Cyclophosphamide versus cyclosporine A therapy in steroid-resistant nephrotic syndrome: a retrospective study with a mean 5-year follow-up. J Int Med Res. 2018; 46(11):4506-17.
33. Lombel RM, Gipson DS, Hodson EM. Treatment of steroid-sensitive nephrotic syndrome: new guidelines from KDIGO. Pediatr Nephrol. 2013; 28(3):415-26.
34. Ravani P, Rossi R, Bonanni A, Quinn RR, Sica F, Bodria M, Pasini A, Montini G, Edefonti A, Belingheri M, De Giovanni D, Barbano G, Degl'Innocenti L, Scolari F, Murer L, Reiser J, Fornoni A, Ghiggeri GM. Rituximab in Children with Steroid-Dependent Nephrotic Syndrome: A Multicenter, Open-Label, Noninferiority, Randomized Controlled Trial. J Am Soc Nephrol. 2015; 26(9):2259-66.
35. Ravani P, Magnasco A, Edefonti A, Murer L, Rossi R, Ghio L, Benetti E, Scozzola F, Pasini A, Dallera N, Sica F, Belingheri M, Scolari F, Ghiggeri GM. Short-term effects of rituximab in children with steroid- and calcineurin-dependent nephrotic syndrome: a randomized controlled trial. Clin J Am Soc Nephrol. 2011; 6(6):1308-15.
36. Ruggenenti P, Ruggiero B, Cravedi P, Vivarelli M, Massella L, Marasa M, Chianca A, Rubis N, Ene-Iordache B, Rudnicki M, Pollastro RM, Capasso G, Pisani A, Pennesi M, Emma F, Remuzzi G. Rituximab in steroid-dependent or frequently relapsing idiopathic nephrotic syndrome. J Am Soc Nephrol. 2014; 25(4):850-63.
37. Sun L, Xu H, Shen Q, Cao Q, Rao J, Liu HM, Fang XY, Zhou LJ. Efficacy of rituximab therapy in children with refractory nephrotic syndrome: a prospective observational study in Shanghai. World J Pediatr. 2014; 10(1):59-63.
38. Larkins NG, Liu ID, Willis NS, Craig JC, Hodson EM. Non-corticosteroid immunosuppressive medications for steroid-sensitive nephrotic syndrome in children. Cochrane Database Syst Rev. 2020; 4:CD002290.
39. Mundel P, Shankland SJ. Podocyte biology and response to injury. J Am Soc Nephrol. 2002; 13(12):3005-15.
40. Lim BJ, Yang HC, Fogo AB. Animal models of regression/progression of kidney disease. Drug Discov Today Dis Models. 2014; 11:45-51.
41. Pippin JW, Brinkkoetter PT, Cormack-Aboud FC, Durvasula RV, Hauser PV, Kowalewska J, Krofft RD, Logar CM, Marshall CB, Ohse T, Shankland SJ. Inducible rodent models of acquired podocyte diseases. Am J Physiol Renal Physiol. 2009; 296(2):F213-29.
42. Eto N, Wada T, Inagi R, Takano H, Shimizu A, Kato H, Kurihara H, Kawachi H, Shankland SJ, Fujita T, Nangaku M. Podocyte protection by darbepoetin: preservation of the cytoskeleton and nephrin expression. Kidney Int. 2007; 72(4):455-63.
43. Ransom RF, Lam NG, Hallett MA, Atkinson SJ, Smoyer WE. Glucocorticoids protect and enhance recovery of cultured murine podocytes via actin filament stabilization. Kidney Int. 2005; 68(6):2473-83.
44. Has C, Spartà G, Kiritsi D, Weibel L, Moeller A, Vega-Warner V, Waters A, He Y, Anikster Y, Esser P, Straub BK, Hausser I, Bockenhauer D, Dekel B, Hildebrandt F, Bruckner-Tuderman L, Laube GF. Integrin

α3 mutations with kidney, lung, and skin disease. The New England Journal of Medicine. 2012; 366(16):1508–14.

45. Hara M, Yanagihara T, Kihara I. Urinary podocytes in primary focal segmental glomerulosclerosis. Nephron. 2001; 89(3):342-7.
46. Kim YH, Goyal M, Kurnit D, Wharram B, Wiggins J, Holzman L, Kershaw D, Wiggins R. Podocyte depletion and glomerulosclerosis have a direct relationship in the PAN-treated rat. Kidney Int. 2001; 60(3):957-68.
47. Goto H, Wakui H, Komatsuda A, Ohtani H, Imai H, Sawada K, Kobayashi R. Renal alpha-actinin-4: purification and puromycin aminonucleoside-binding property. Nephron Exp Nephrol. 2003; 93(1):e27-35.
48. Schiffer M, Bitzer M, Roberts IS, Kopp JB, ten Dijke P, Mundel P, Bottinger EP. Apoptosis in podocytes induced by TGF-beta and Smad7. J Clin Invest. 2001; 108(6):807-16.
49. Matovinović MS. 3. Podocyte Injury in Glomerular Diseases. EJIFCC. 2009; 20(1):21-7
50. Liapis H, Romagnani P, Anders HJ. New insights into the pathology of podocyte loss: mitotic catastrophe. Am J Pathol. 2013; 183(5):1364–74.
51. Takahashi Y, Ikezumi Y, Saitoh A. Rituximab protects podocytes and exerts anti-proteinuric effects in rat adriamycin-induced nephropathy independent of B-lymphocytes. Nephrology (Carlton). 2017; 22(1):49-57.
52. Cittera E, Onofri C, D'Apolito M, Cartron G, Cazzaniga G, Zelante L, Paolucci P, Biondi A, Introna M, Golay J. Rituximab induces different but overlapping sets of genes in human B-lymphoma cell lines. Cancer Immunol Immunother. 2005; 54(3):273-86.
53. Matsusaka T, Sandgren E, Shintani A, Kon V, Pastan I, Fogo AB, Ichikawa I. Podocyte injury damages other podocytes. J Am Soc Nephrol. 2011; 22(7):1275-85.
54. Trimarchi H. Podocyturia: Potential applications and current limitations. World J Nephrol. 2017; 6(5):221-8.
55. Chan HT, Hughes D, French RR, Tutt AL, Walshe CA, Teeling JL, Glennie MJ, Cragg MS. CD20-induced lymphoma cell death is independent of both caspases and its redistribution into triton X-100 insoluble membrane rafts. Cancer Res. 2003; 63(17):5480-9.
56. Ghetie MA, Bright H, Vitetta ES. Homodimers but not monomers of Rituxan (chimeric anti-CD20) induce apoptosis in human B-lymphoma cells and synergize with a chemotherapeutic agent and an immunotoxin. Blood. 2001; 97(5):1392-8.
57. Golay J, Zaffaroni L, Vaccari T, Lazzari M, Borleri GM, Bernasconi S, Tedesco F, Rambaldi A, Introna M. Biologic response of B lymphoma cells to anti-CD20 monoclonal antibody rituximab in vitro: CD55 and CD59 regulate complement-mediated cell lysis. Blood. 2000; 95(12):3900-8.
58. Ahmad A, Mitrofanova A, Bielawski J, Yang Y, Marples B, Fornoni A, Zeidan YH. Sphingomyelinase-like phosphodiesterase 3b mediates radiation-induced damage of renal podocytes. Faseb J. 2017; 31(2):771-80.

59. Frisch SM, Screaton RA. Anoikis mechanisms. Curr Opin Cell Biol. 2001; 13(5):555-62.
60. Finlay D, Vuori K. Novel noncatalytic role for caspase-8 in promoting SRC-mediated adhesion and Erk signaling in neuroblastoma cells. Cancer Res. 2007; 67(24):11704-11.
61. Senft J, Helfer B, Frisch SM. Caspase-8 interacts with the p85 subunit of phosphatidylinositol 3-kinase to regulate cell adhesion and motility. Cancer Res. 2007; 67(24):11505-9.

Tables

Table 1: Number of podocyte actin stress fibers

	Number of actin stress fibers: Mean ±SD [%]		
	Healthy actin stress fiber appearance	Reduced number of actin stress fibers	No actin stress fibers
Control	89.6 ± 5.2	7.6 ± 3.7	2.8 ± 1.6
RTX	90.1 ± 3.1	6.4 ± 1.7	3.5 ± 1.5
PAN	2.0 ± 0.8	10.2 ± 2.0	87.7 ± 2.5
PAN + RTX	10.0 ± 1.9	14.0 ± 4.7	75.9 ± 6.0

To evaluate the integrity of the actin cytoskeleton podocytes were divided into three groups: "healthy actin stress fiber appearance", "reduced number of actin stress fibers" and "no actin stress fibers". RTX = rituximab; PAN = puromycin aminonucleoside; n = 4 experiments; ≥ 25 images per condition. Data are means (%) ± SD.

Table 2: Number of apoptotic podocytes

Number of apoptotic podocytes: Mean ±SD [%]			
Control	RTX	PAN	PAN + RTX
0.6 ± 1.2	0.4 ± 0.8	23.3 ± 8.7	12.5 ± 6.8

Hoechst nuclear staining was performed for the detection of apoptosis. Apoptotic cells were defined as percentage of fragmented nuclei. RTX = rituximab; PAN = puromycin aminonucleoside; n = 4 experiments; ≥ 200 cells per condition. Data are means (%) ± SD.

Table 3: Podocyte Caspase activity levels

Caspase activity levels: Mean ±SD [%]				
	Control	RTX	PAN	PAN + RTX
Caspase-8	1.0 ± 0.0	1.3 ± 0.2	7.2 ± 2.8	1.7 ± 0.3
Caspase-3	1.0 ± 0.0	1.4 ± 0.4	19.0 ± 12.7	2.7 ± 2.0

Cleaved Caspase-8 and -3 activity levels were measured by Western-blot analysis for the detection of apoptosis. RTX = rituximab; PAN = puromycin aminonucleoside; n = 3 experiments; Data are means (%) ± SD.

Table 4: Podocyte adhesion efficiency

Cell size: Mean ±SD [µm²]				
	Control	RTX	PAN	PAN + RTX
1 hour	6860 ± 5048	6580 ± 4971	4285 ± 3393	6343 ± 4619
6 hours	12562 ± 11023	12965 ± 11371	5350 ± 4027	10173 ± 8421

Quantification of cell size as a means of determining adhesion efficiency at 1 and 6 hours after post plating. RTX = rituximab; PAN = puromycin aminonucleoside; n = 4 experiments; ≥ 300 cells per condition. Data are means (%) ± SD.

Figures

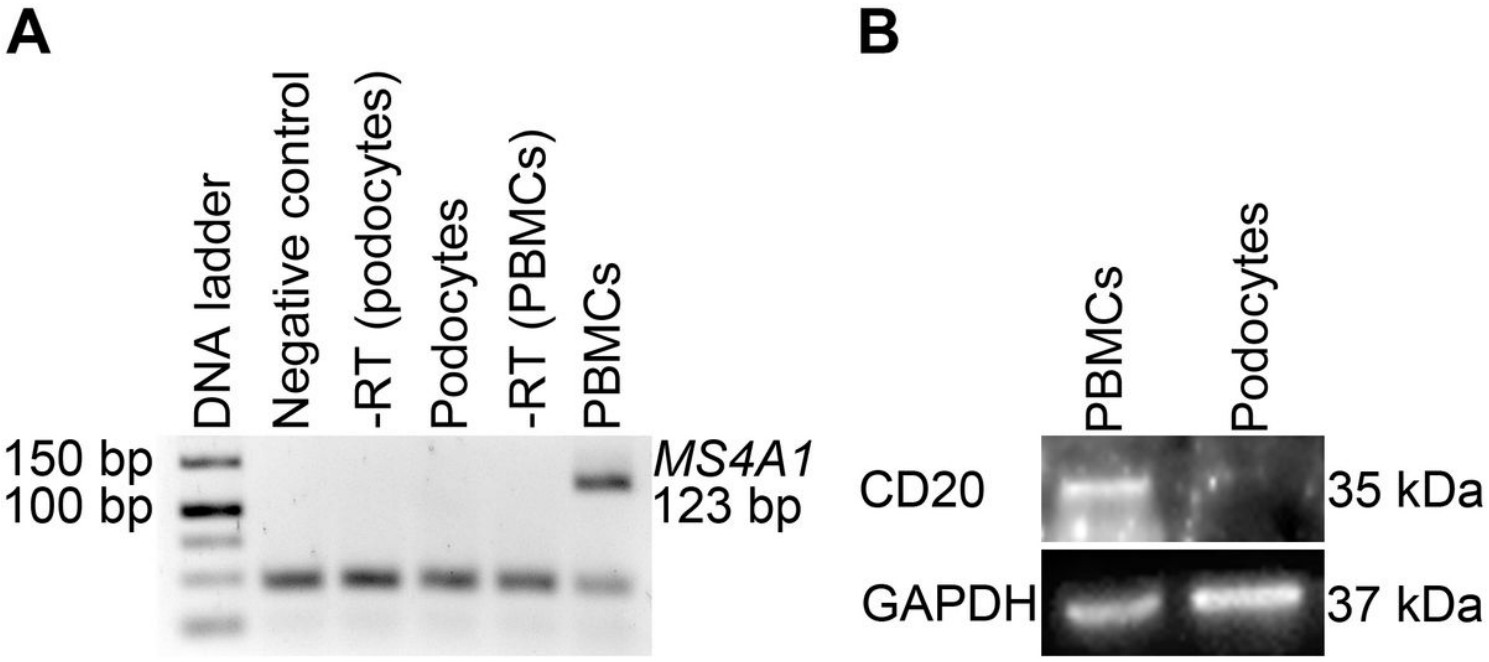

Figure 1

Human podocytes do not express CD20 (A) RT-PCR analysis for MS4A1. Negative control = negative amplification control with nuclease-free water; -RT = negative amplification control without reverse transcriptase; +RT = cDNA with reverse transcriptase. (B) Western-blot analysis for CD20. RTX was used as primary antibody against CD20. GAPDH = loading control; PBMCs = peripheral blood mononuclear cells; RTX = rituximab.

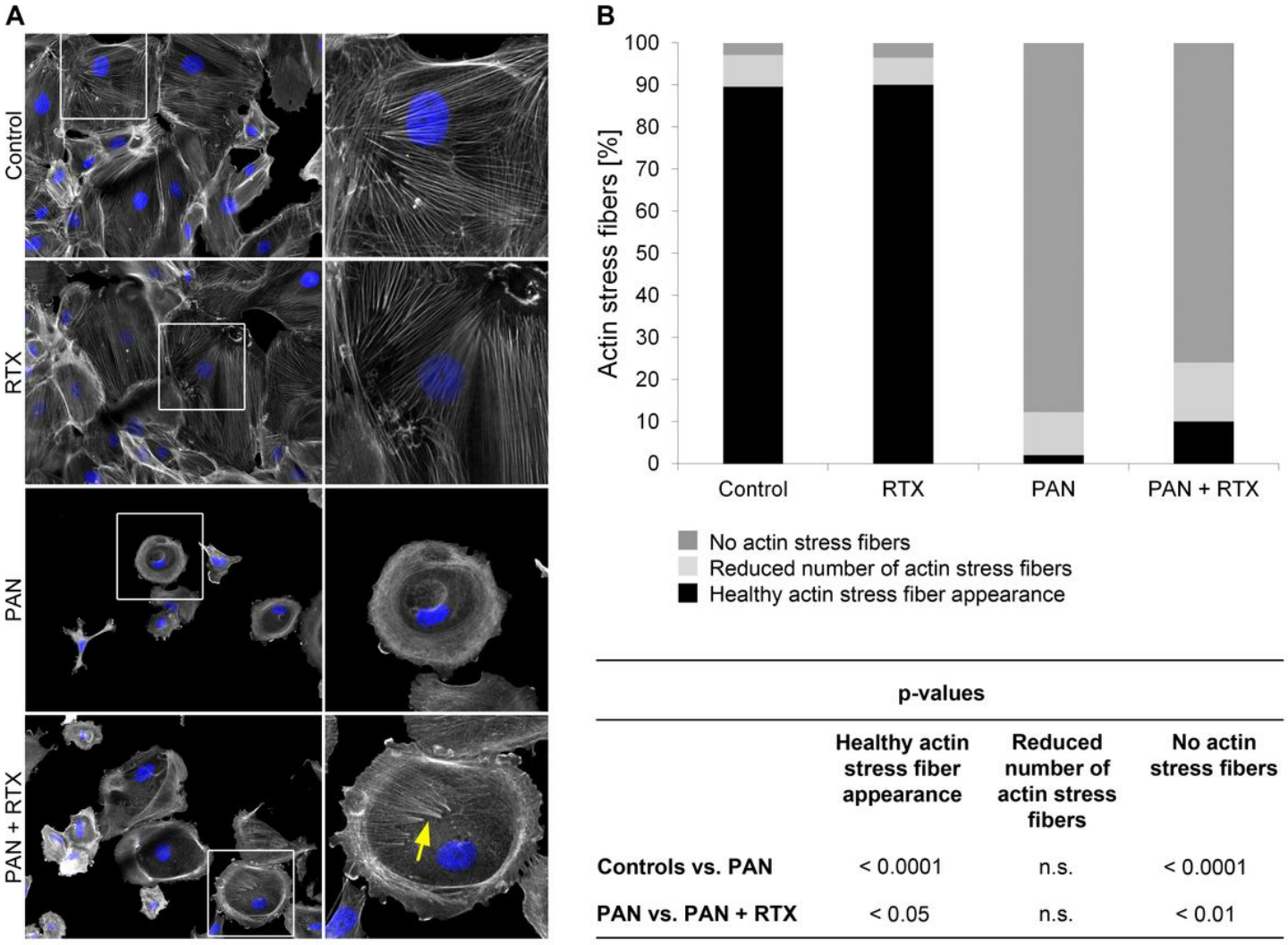

p-values			
	Healthy actin stress fiber appearance	**Reduced number of actin stress fibers**	**No actin stress fibers**
Controls vs. PAN	< 0.0001	n.s.	< 0.0001
PAN vs. PAN + RTX	< 0.05	n.s.	< 0.01

Figure 2

Rituximab prevents disruption of the actin cytoskeleton in human podocytes (A) Actin (phalloidin-TRITC, grey) and nuclear staining (DAPI, blue) of human podocytes. Scale bar = 50 µm. (B) Number of central actin stress fibers [%]. For classification podocytes were divided into three groups: "healthy actin stress fiber appearance", "reduced number of actin stress fibers" and "no actin stress fibers". Statistics: One-way ANOVA with Tukey's multiple comparisons test; the mean ± SD is shown [%]. n = 4 experiments; ≥ 25 images per condition. n.s. = not significant. RTX = rituximab; PAN = puromycin aminonucleoside.

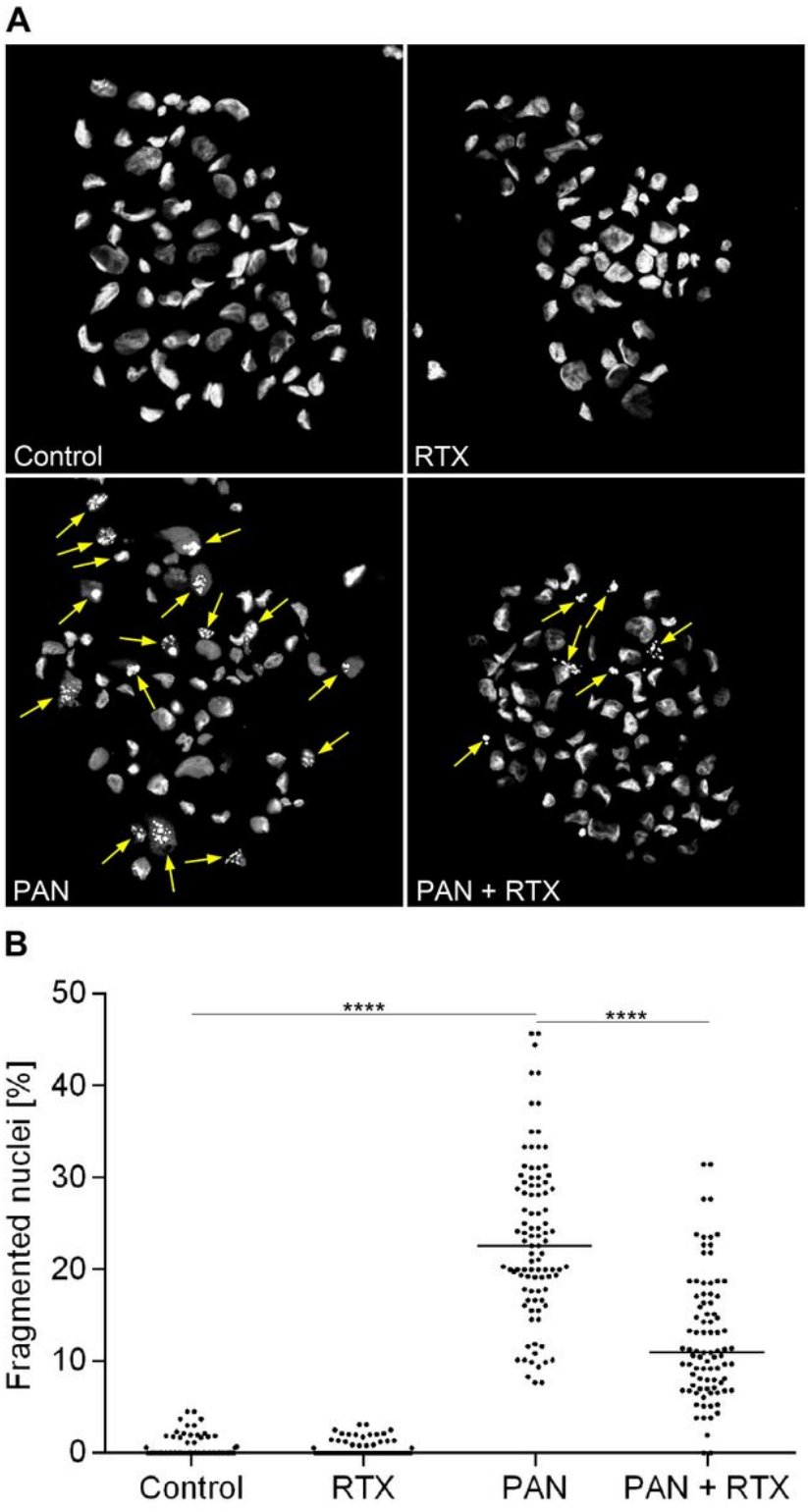

Figure 3

Rituximab prevents podocyte apoptosis (Hoechst nuclear staining) Hoechst nuclear staining was performed for the detection of apoptosis. Apoptotic cells were defined as percentage of fragmented nuclei. (A) Nuclear staining (DAPI, grey) of human podocytes. Scale bar = 50 µm. (B) Number of apoptotic podocytes [%]. Statistics: One-way ANOVA with Tukey's multiple comparisons test; the median [%] is

shown; **** = p < 0.0001; n = 4 experiments; ≥ 200 cells per condition. RTX = rituximab; PAN = puromycin aminonucleoside.

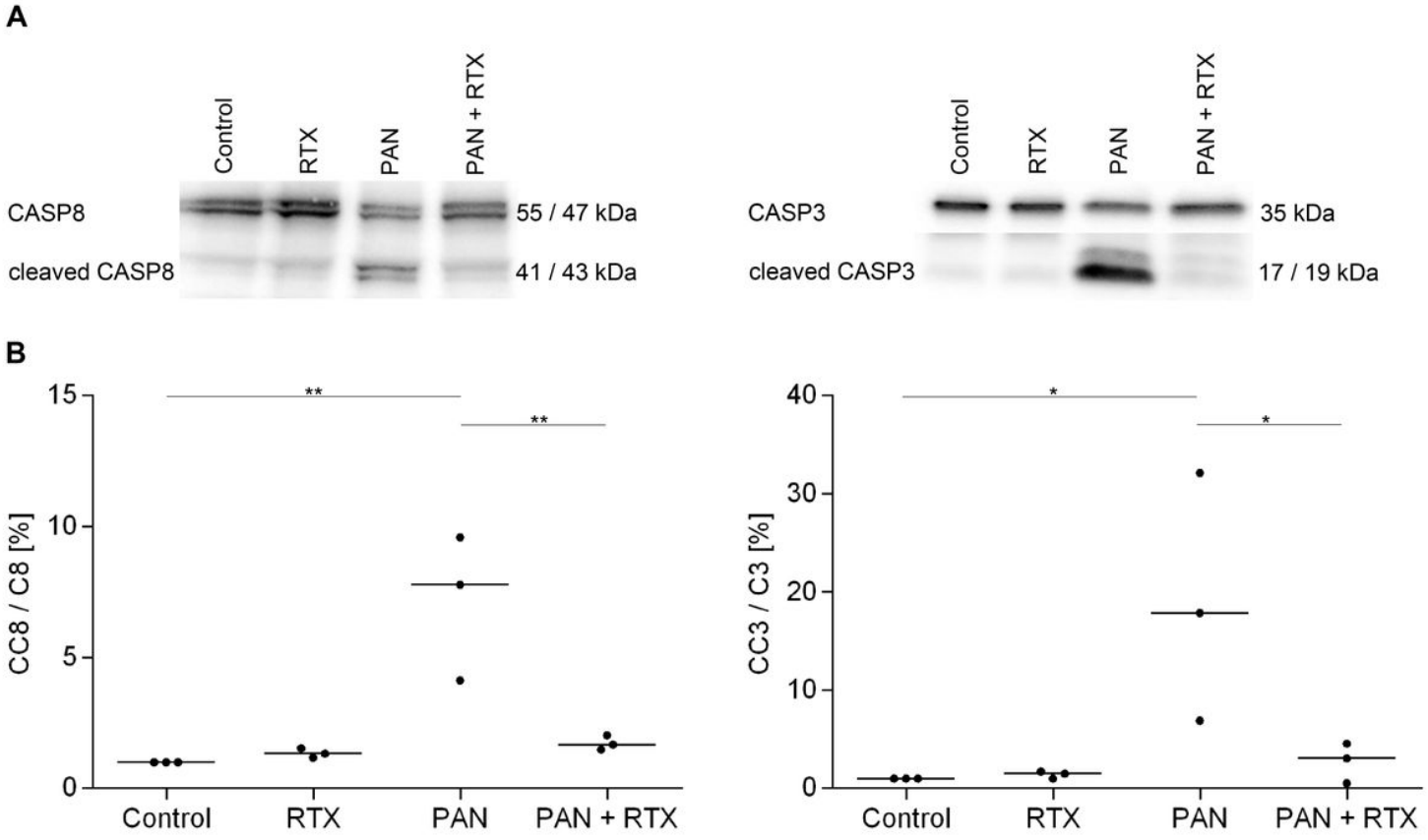

Figure 4

Rituximab prevents podocyte apoptosis (Caspase Western-blots). Western blot analysis to measure the activation levels of Caspase-8 and -3 (representative example from 3 independent experiments). Caspase-8 and -3 = total Caspase protein levels, cleaved Caspase-8 and -3 = active Caspase proteins. (B) For quantification the amount of active cleaved Caspase proteins were normalized with respect to total Caspase levels. Statistics: One-way ANOVA with Tukey's multiple comparisons test; the median [%] is shown; * = p <0.05; ** = p <0.01; n = 3 experiments. CC8 = cleaved Caspase-8; C8 = total Caspase-8; CC3 = cleaved Caspase-3; C3 = total Caspase-3; RTX = rituximab; PAN = puromycin aminonucleoside.

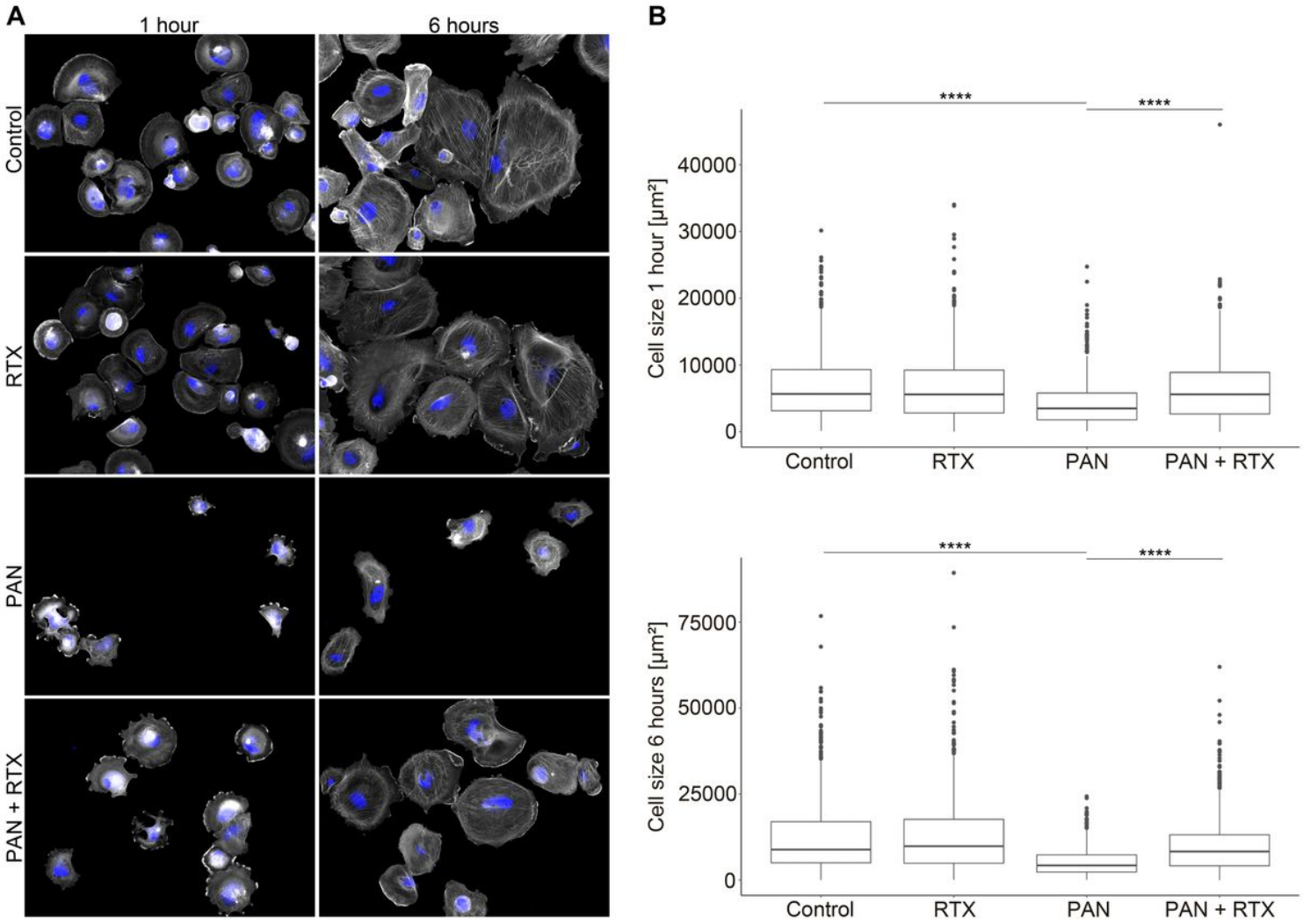

Figure 5

Rituximab enhances podocyte adhesion (A) Actin (phalloidin-TRITC, grey) and nuclear (DAPI, blue) staining at 1 and 6 hours after post plating. Scale bar = 50 µm. (B) Quantification of cell size 1 and 6 hours after post plating. Statistics: Kruskal-Wallis test with Dunn's multiple comparisons test; the median is shown. **** = $p < 0.0001$; n = 4 experiments; ≥ 300 cells per condition. RTX = rituximab; PAN = puromycin aminonucleoside.